



Research article

Enzyme-like denitrification with an oxidorhenium(V) complex: reduction of nitrite to N₂O

Fabian Wiedemaier^{a,1}, David M. Köpfler^{a,2}, Christian Schlegl^{a,2}, Christof Holzer^b,
Ferdinand Belaj^a, Nadia C. Mösch-Zanetti^{a,*}, Jörg A. Schachner^{a,*}

^a Institute of Chemistry, University of Graz, Schubertstr. 1, 8010 Graz, Austria

^b Institute of Quantum Materials and Technologies, Karlsruhe Institute of Technology, P.O. Box 3640, 76021 Karlsruhe, Germany

ARTICLE INFO

Keywords:

Homogeneous catalysis
Rhenium complexes
Bio-mimetic
Reduction
Nitrate

ABSTRACT

Ever-growing levels of nitrate are threatening a constantly diminishing natural resource, namely drinking water. With the Haber-Bosch process ensuing industrial-scale production of nitrate for artificial fertilizers, mankind is significantly interfering with the global nitrogen cycle. While nature can solve the problem via a cascade of nitrate reducing enzymes, there is no comparable technology available, due to a fundamental lack of scientific knowledge. We have developed oxidorhenium(V) complex [ReOCl(L1)₂] (1), that not only catalytically reduces NO₃⁻ to NO₂⁻ and NO under ambient, aqueous conditions, but is the first example of a catalyst to also catalytically reduces NO further to N₂O, thereby mirroring the pathway of biological, enzymatic denitrification of NO₃⁻. DFT calculations support a mechanism a reductive coupling of an NO molecule to a Re-nitrosyl complex to give an intermediate Re-(κ²-O₂N₂²⁻) hyponitrite complex.

The reduction of nitrite occurs via a single electron transfer, yielding NO and paramagnetic dioxidorhenium(VI) complex [ReO₂(L1)₂] (2'). Neutral complex 2' is not catalytically active anymore, but addition of [Cu(II)Cl₂] oxidizes complex 2' back into the catalytically active cationic complex [ReO₂(L1)₂]⁺ (2), thereby closing the catalytic cycle. In addition, we could identify the decomposition products of 2', namely complex [ReO(L1)₂][ReO₄] (3a) and of 2, namely complex (H₂L1)[ReO₄] (3b). The kinetics of formation of both 2' and 2 as well as their respective decomposition products 3a and 3b were studied by UV-Vis spectroscopy and electrochemistry.

1. Introduction

Biological denitrification occurs via an anaerobic pathway, by which many microbial species gain energy to support the oxidative phosphorylation of ATP in the absence of oxygen [1]. In the four-step, five-electron cascade, NO₃⁻ is reduced to N₂. Together with nitrogen fixation (N₂ → NH₄⁺) and nitrification (NH₄⁺ → NO₃⁻), denitrification is an important part of the global nitrogen cycle [1–4]. In bacteria, the four steps of denitrification (NO₃⁻ → NO₂⁻ → NO → N₂O → N₂) are catalyzed by metalloenzymes (most commonly) containing Mo (*nitrate reductase*, NAR), Cu (*nitrite reductase*, NIR), Cu/Fe (*nitric oxide reductase*, NOR) and Cu (*nitrous oxide reductase*, NOS) [2].

Man-made nitrogen input into the environment has nearly doubled since pre-industrial times due to the extensive use of nitrate in agriculture as fertilizer [3]. The high water solubility of nitrate salts causes its

buildup in ground water. Nitrate, as well as nitrite and ammonium, is a regulated pollutant of drinking water [5], with a set maximum level of 50 ppm in the “Groundwater Directive” by the EU [6]. High nitrate concentrations in drinking water are potentially linked to severe health effects, including certain forms of cancer [7].

Early examples of nitrate reduction complexes were published in 1980 by Topich, describing a tethered, sulfur-coordinated Mo(VI) complex [8] and later on by Tacke and coworkers, using a heterogeneous Pd/Cu catalyst [9]. Thereafter, the field of heterogeneous catalytic nitrate reduction has evolved significantly [5,10–13]. The first example of homogeneous reduction of nitrate with a rhenium complex was published in 1996 by Espenson [14]. The authors reported that methyldioxidorhenium, [CH₃ReO₂], is capable to reduce nitrate anions at pH = 0 with hypophosphorous acid, H₃PO₂, as sacrificial reductant. The bio-mimetic molybdenum model complex [Mo(SPh)(PPh₃)(mnt)₂]⁻

* Corresponding authors.

E-mail addresses: nadia.moesch@uni-graz.at (N.C. Mösch-Zanetti), joerg.schachner@uni-graz.at (J.A. Schachner).

¹ Present address: Lonza Group AG, 3930 Visp, Switzerland.

² Present address: Insort GmbH, 8324 Kirchberg an der Raab, Austria.

(mnt²⁻ = 1,2-dicyanoethylenedithiolate), reported in 2006, showed 30 catalytic turnovers with NO₃⁻ using PPh₃ as reductant. However, when [Mo(SPh)(PPh₃)(mnt)₂]⁻ reacts with NO₂⁻, the formation of NO leads to the catalytically inactive nitrosyl-complex [Mo(NO)₂(mnt)₂]²⁻ (Scheme 1, a) [15].

In 2016, the group of Fout published a bio-inspired, air-sensitive iron complex with a tripodal, tetradentate azafulvene-amine ligand [16]. This iron complex showed catalytic activity to reduce both ClO₄⁻ (TON = 3) or NO₃⁻ (TON = 3.5). Furthermore, in nitrate reduction, also an inactive iron-nitrosyl complex is formed (Scheme 1, b). Very recently, the same group found an elegant solution to further reduce NO. By adjusting the reaction conditions, the formation of the catalytically inactive iron-nitrosyl complex can be avoided and the gaseous NO is instead reduced to N₂O by addition of PPh₃ [17]. Another example are a set of bio-inspired Mo catalysts recently reported by our group, equipped with *S,N*-bidentate thio-pyridine (SPy) or thio-pyrimidine (SPym) ligands, which showed moderate catalytic activity for nitrate reduction, but eventually also observed the formation of stable Mo-nitrosyl complexes, which prevented further reduction (Scheme 1, c) [18]. Therefore, NO can be viewed as a catalyst poison by formation of stable nitrosyl complexes, which must be prevented in active catalytic systems. Two very recent reviews summarize metal-catalyzed nitrate reductions [19].

In contrast to the aforementioned examples, only two other metal complexes have so far shown catalytic activity for the reduction of NO. The first example came from the group of Lee in 2019, where a PNP-pincer complex of Ni showed full reduction of NO₃⁻ to N₂ [20]. The intermediately formed (PNP)Ni-NO complex thereby catalyzed the disproportionation of both NO to N₂O as well as N₂O to N₂ (Scheme 2, a). The second example is rare trinuclear copper cluster, supported by tethered NHC-ligands (Scheme 2, b), published in 2025 by Buss and co-worker [21]. The cluster shows OAT-reactivity to all relevant N-oxides and can be regenerated by the diborane B₂Pin₂, thereby enabling high catalytic turnovers for NO and N₂O. The newest example is our previously reported oxidorhenium(V) complex [ReOCl(L1)₂] (1) (Scheme 2, c), coordinated by two dimethyloxazoline-phenolato ligands dmoz), which exhibits good activity in both perchlorate reduction [22] and nitrate reduction [23] catalysis with dimethyl sulfide (SMe₂) as the sacrificial oxygen atom acceptor.

A particular asset of our system is its robustness as inert reaction conditions are not required due to the stability of 1 towards moisture and oxygen. We demonstrated that 1 reacts with nitrate to the cationic, catalytically active dioxidorhenium(VII) complex [ReO₂(L1)₂]⁺ (2) while with nitrite the neutral, catalytically inactive dioxidorhenium(VI)

complex [ReO₂(L1)₂] (2') is formed (Scheme 3; Scheme 4, a), as evidenced by the isolation of a small amount of single crystals suitable for X-ray diffraction analysis [23].

In a previous investigation, while following a stoichiometric reaction of 1 and ¹⁵NO₃⁻ via ¹⁵N NMR spectroscopy, we were surprised to see ¹⁵N₂O after 3 days, which must be the reduction product of intermediately formed ¹⁵NO [23]. This observation prompted us to further investigate the reduction step of NO. In contrast to the examples described above however, we could not isolate a rhenium nitrosyl complex during the course of our investigations.

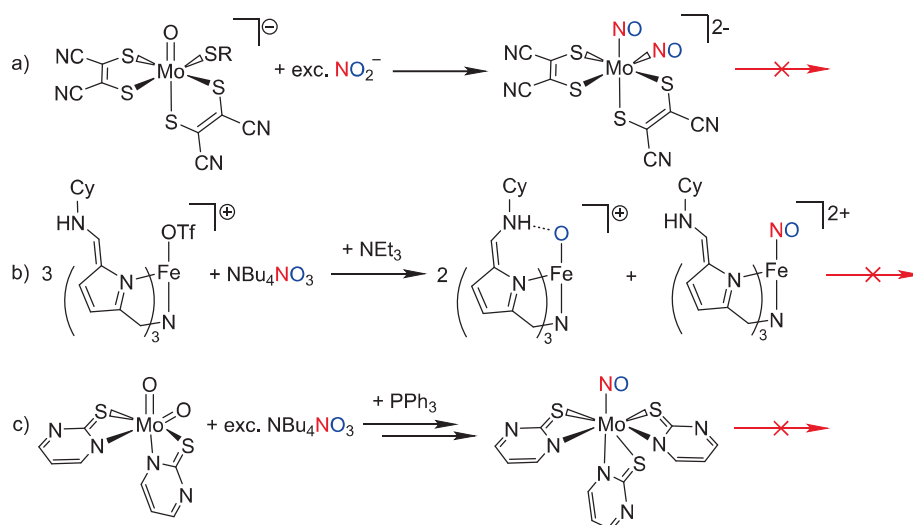
Within this manuscript, a targeted synthesis of catalytically inactive complex [ReO₂(L1)₂] (2') is described, which allowed experiments towards its reactivation by various 1 e⁻ oxidants, identifying [Cu(II)Cl₂] as the most convenient oxidant to turn over the NO₂⁻ to NO cycle (Scheme 4, b). Furthermore, the formation of gaseous NO as the reduction product of NO₂⁻ is confirmed via gas-phase IR spectroscopy. Finally, DFT calculations support an NO reduction mechanism via the intermediate formation of a Re-hyponitrite (= κ²-O₂N₂²⁻) complex.

The here presented mechanistic insights deliver crucial information on how to solve the challenges posed to an effective biomimetic catalyst for nitrate reduction, which has to overcome catalyst deactivation by 1 e⁻ OAT steps as well as irreversible coordination of NO, in order to be a mutual catalyst for nitrate, nitrite and NO reduction. Based on the formation of N₂O, potentially dinitrogen can be obtained as the final product, rendering catalyst 1 truly biomimetic.

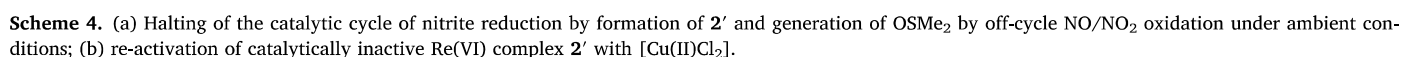
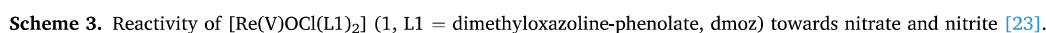
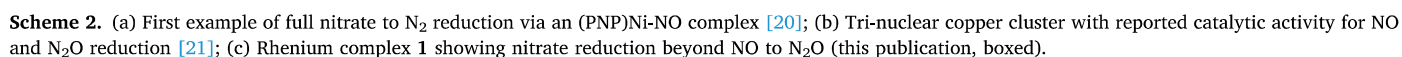
Finally, for both complexes 2' and 2, thermodynamic and kinetic data of their respective formation as well as decomposition were obtained and their respective decomposition products could be identified as complexes [ReO(L1)₂][ReO₄] (3a) and (H₂L1)[ReO₄] (3b), respectively (see SI).

2. Results and discussion

Complex [ReO₂(L1)₂] (2') was synthesized by reacting AgNO₂ with 1 in acetonitrile at room temperature (Scheme S2, a), resulting in a color change from initially green to golden-brown within minutes. Work-up and purification by flash chromatography (silica/Et₃N, CH₂Cl₂) gave complex 2' as a light-brown powder in up to 64 % yield (see SI). Quick work-up is important, as 2' is moisture sensitive when dissolved, which is indicated by the gradual disappearance of the golden-brown color. The ¹H NMR spectrum reflects the paramagnetism of 2', where all the peaks are broadened, and the signals for the four methyl groups are shifted downfield to 22.4, 17.7 and 11.5 ppm (Fig. S4). A Gouy balance measurement of 2' found a μ_{eff} = 1.52 BM. However, an EPR spectrum



Scheme 1. (a)–(c) Complexes capable of nitrate reduction to NO, however forming catalytically inactive nitrosyl complexes [15,16,18].



$E_{1/2}$ potential of **2'** is relatively low [25]. The measured potential also explains the lack of oxidation activity against SMe_2 (vide infra), which shows an oxidation potential of $E_{\text{ox}} = 1.45$ V in acetonitrile [26]. Variation of the scan-rate did not change the ratio of the anodic and the cathodic peak indicating a rather long-lived species, which is in line with

kinetic measurements (see SI). In the solid state, **2'** is stable towards ambient atmosphere.

2.1. Decomposition pathways

By stoichiometric oxidation reactions with various 1 e^- (e.g. NO_2^-) or 2 e^- oxidants (e.g. NO_3^- , pyridine-*N*-oxide, TBHP, see SI), the kinetics of formation and subsequent decomposition of paramagnetic, neutral Re(VI) complex **2'** and cationic Re(VII) complex **2** was studied by UV–Vis spectroscopy and electrochemistry (Table S1). By UV–Vis spectroscopy, a half-life time of complex **2'** in $\text{CH}_3\text{CN}/\text{H}_2\text{O}$ (95/5 vol%) of 86 h was determined. Complex **2'** decomposes via disproportionation to ionic Re(V)/Re(VII) complex $[\text{ReO}(\text{L}1)_2][\text{ReO}_4]$ (**3a**, Scheme S2, b). Also, by UV–Vis, a half-life time of cationic complex **2** of app. 2 h in CH_3CN was measured. Complex **2** decomposes by hydrolysis with H_2O to ionic complex $(\text{H}_2\text{L}1)[\text{ReO}_4]$ (**3b**) (Scheme S3, b). For both complexes **3a** and **3b**, the solid state structures could be obtained by single-crystal X-ray diffraction (Fig. S3, Table S2).

The other product in the synthesis of **2'** is NO. To confirm, the resulting volatiles of the synthesis of **2'** were analyzed via gas-phase IR spectroscopy. The experimental set-up is shown in Fig. S1. Under inert conditions, the volatile products of the synthesis of **2'** were purged with a slow N_2 -flow into the attached gas-cell of the IR spectrometer, resulting in the typical gas phase spectrum of NO, with the P and R branch centered around 1880 cm^{-1} , as shown in Fig. 1, which confirms the formation of NO [27]. We can now confirm that NO_2^- is indeed reduced by only one electron to NO, similar to the enzymatic reaction.

NO is easily oxidized by air to gaseous NO_2 , a strong oxidizing agent capable to oxidize SMe_2 to OSMe_2 (Scheme S1) [28]. As the catalytic performance of our Re catalyzed nitrate or nitrite reductions with SMe_2 was generally determined by ^1H NMR detection of the formed OSMe_2 , this off-cycle production of OSMe_2 leads to problems with determining the true TON of the catalyst (Scheme 3, a). Therefore, all NO_3^- reduction experiments had to be performed under inert atmosphere.

With singly oxidized, paramagnetic Re(VI) complex **2'** in hand, we now could further investigate the chemical properties of **2'**, especially with regard to its redox chemistry and a potential restoration of catalytic activity. The low oxidation potential of **2'** of +110 mV in principle allows for a wide range of 1 e^- oxidants, thereby re-generating catalytically active Re(VII) cation **2** again. Inspired by the Wacker process, we

tested both anhydrous $[\text{Cu}(\text{II})\text{Cl}_2]$ as well as $[\text{Cu}(\text{II})\text{Cl}_2 \cdot 2\text{H}_2\text{O}]$. We were delighted to observe that in both cases, complete consumption of **2'** occurred within 1 h, even though $[\text{Cu}(\text{II})\text{Cl}_2]$ only poorly dissolves in the used acetonitrile/water mixture. Single electron oxidation of **2'** yields the highly reactive, catalytically active Re(VII) cation $[\text{ReO}_2(\text{L}1)_2]^+$ (**2**), which in the presence of SMe_2 clearly gives back Re(V) complex **1** and OSMe_2 . Indeed, we now observed a clean, full conversion of **2'** to **1** and OSMe_2 in under 1 h (Scheme 4, b).

2.2. Reduction of NO in presence of $[\text{ReOCl}(\text{L}1)_2]$ (**1**) and SMe_2

Due to the air sensitivity of NO, the nitrite reduction step has to be done under strict exclusion of O_2 . To test our experimental set-up, **1** was reacted with 1 equiv. of NBu_4NO_2 in presence of 3 equiv. of SMe_2 in a J-Young NMR tube (Fig. 2, a). Surprisingly though, in several experiments, ^1H NMR spectroscopy always revealed a slow oxidation over 400 h of 0.5 equivalents SMe_2 to OSMe_2 (Fig. 2, b), ruling out adventitious oxygen contamination.

A non-linear fit confirmed a boundary value for the OSMe_2 formation of 0.51 ± 0.03 equivalents. The blank reaction with NO and SMe_2 in absence of complex **1**, monitored over 10 days by ^1H NMR spectroscopy, did not yield any OSMe_2 .

We assume that a reductive coupling of two NO molecules occurs, which, after an OAT step, yields 1 equiv. of N_2O and OSMe_2 . Although the reduction of NO in the presence of **1** over 10 days seems to proceed on a rather slow time scale, the uncatalyzed disproportionation of NO at 298 K and 1 atm would take years [29]. Hence, the significant rate acceleration points towards a rhenium-catalyzed NO disproportionation. Such transition-metal catalyzed disproportionations are well known and have the intermediate formation of nitrosyl-complexes in common [30].

2.3. DFT calculations

To understand the binding of NO to the rhenium center, quantum mechanical investigations were performed at the high-level $\omega\text{B97M-D4}$ [31] and the advanced local hybrid functional CHYF [32]. We started from the non-observed nitrosyl complex $[\text{ReO}(\text{NO})(\text{L}1)_2]$ (**1a***) by replacing the negative chlorido ligand in **1** with a neutral NO molecule. The NO molecule therefore takes on the conformation of an NO^- ligand to compensate for the positive charge on the Re complex. This is

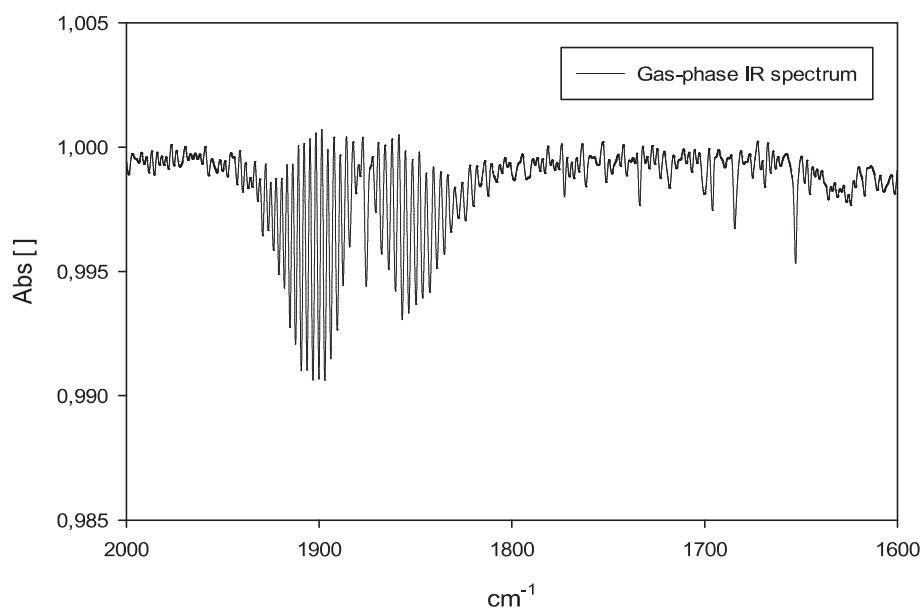


Fig. 1. Gas-phase IR spectrum of the volatiles of an acetonitrile solution of **1** that was reacted with 2.3 equiv. of an aqueous solution of KNO_2 to give **2'** and NO. The observed gas-phase IR spectrum clearly confirms the formation of gaseous NO (P and R branch centered around 1880 cm^{-1}).

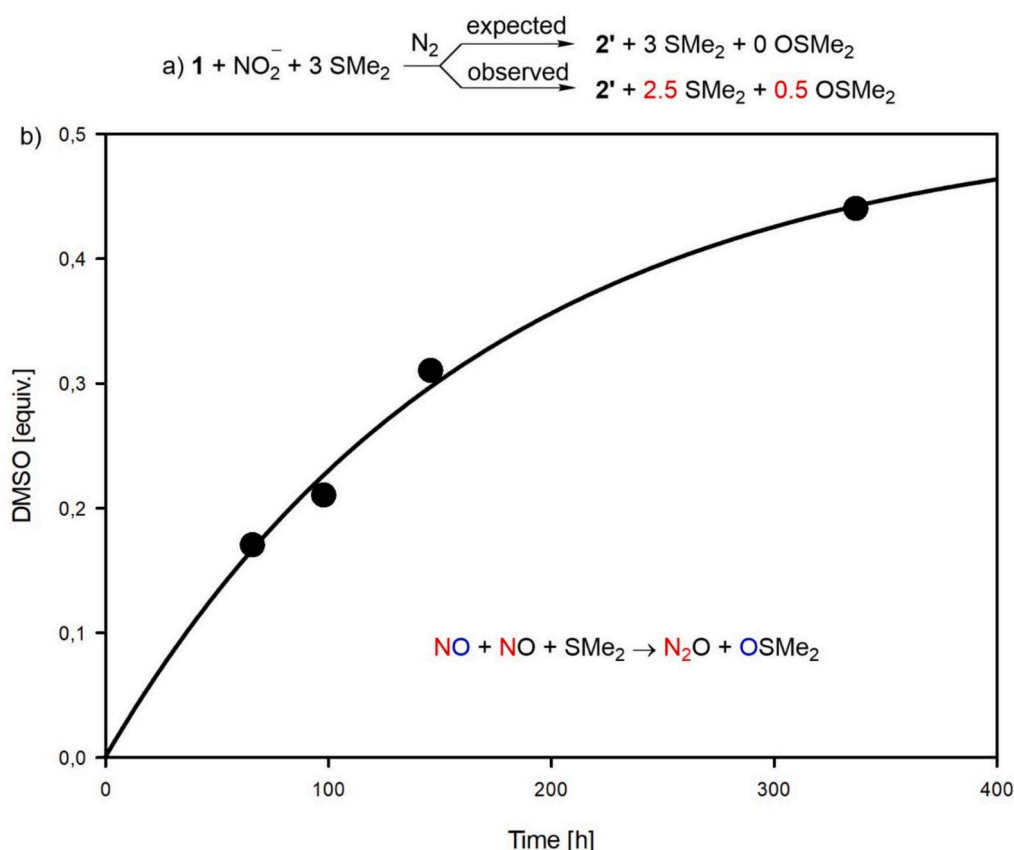


Fig. 2. (a) Nitrite reduction in presence of 1 equiv. of **1** and 3 equiv. of SMe_2 under inert conditions as followed by ^1H NMR spectroscopy: expectation vs. observation; (b) conversion of SMe_2 to OSMe_2 ; conditions: 1 equiv. **1** + 1 equiv. NBu_4NO_2 + 3 equiv. SMe_2 were mixed under inert conditions in a J-Young NMR tube which was sealed immediately afterwards.

reflected by the unusual small angle of $\angle(\text{Re1-N1-O1}) = 88.5^\circ$ (**1a***, Fig. 3, left), which could be regarded as an intermediate state between bent and side-on coordination (bent M-NO : $\sim 120^\circ$; side-on M-NO : $\sim 70^\circ$) [33]. Together with the elongated N1-O1 bond length calculated at 1.265 Å, this bonding situation points to strongly reduced NO^- ligand [33]. An initial coordination of the NO molecule to the oxygen atom of the Re-O bond was also considered, but optimizations lead to no feasible structure. Both functionals predict a thermodynamic highly favorable binding of NO to the vacant coordination site on Re by -194 kJ/mol (wb97M-D4) or -261 kJ/mol (CHYF). We also modelled a nitrosyl complex with an almost linear Re-NO angle, but found it to be 148 kJ/mol higher in energy compared to **1a*** (Fig. S15). At the approach of a second NO molecule (**1b***, Fig. 3, middle) the coordinated nitrosyl

ligand takes on a more typical bent coordination ($\angle(\text{Re1-N1-O1}) = 146.25^\circ$), while the approaching NO molecule does not interact yet with the nitrosyl ligand ($d(\text{N1-N2}) = 1.974$ Å). This is additionally evidenced by the respective N-O distances, which is elongated in the bound nitrosyl ligand (N1-O1 1.179 Å) and almost undisturbed in the approaching NO molecule (N2-O2 1.128 Å; free NO : 1.154 Å [34]). An analysis of the molecular Hessian identifies this species as a local minimum. The transition state of the actual coupling of the second NO molecule could not be investigated computationally, as the shallow potential energy surfaces obtained currently prevents us from determining a more detailed reaction mechanisms *in silico*.

The next identifiable intermediate is formally a $\text{Re(VII)}-(\kappa^2\text{-O}_2\text{N}_2^-)$ hyponitrite complex (**1c***, Fig. 3, right). The $\text{N}_2\text{O}_2^{2-}$ ligand has

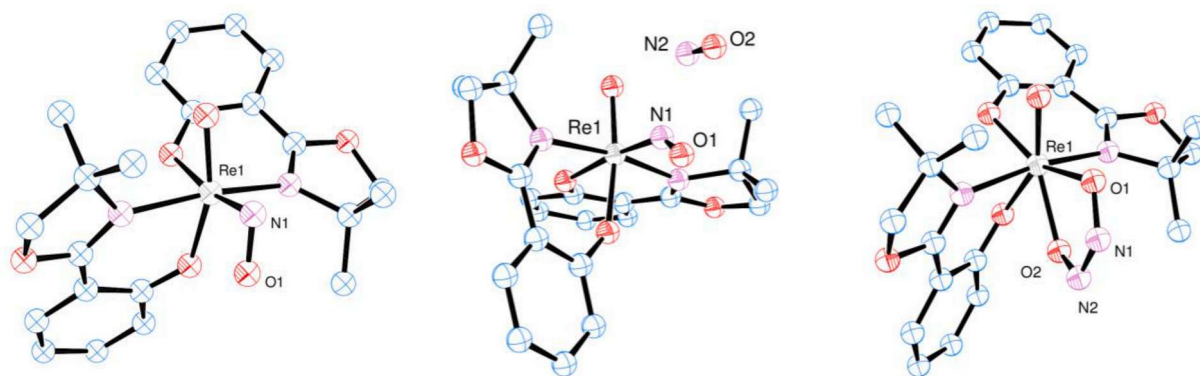


Fig. 3. Calculated structures of strongly bent Re-NO complex **1a*** (left), approach of second NO molecule **1b*** (middle) and $\text{Re-(O}_2\text{N}_2)$ hyponitrite complex **1c*** (right).

rearranged to a κ -O bonding mode. The formation of such coordinated hyponitrite $\text{N}_2\text{O}_2^{2-}$ ligands via reductive coupling of two NO molecules has been previously described in literature [33,35]. The doubly reduced nature of the hyponitrite ligand $\text{N}_2\text{O}_2^{2-}$ is reflected by the calculated short N1-N2 bond distance of 1.249 Å, representing double bond character. In other isolated hyponitrite complexes, the measured N-N bond distance was, for example, 1.235(2) Å [33]. Also, the hyponitrite ligand in **1c*** is almost planar, with a calculated dihedral angle of $\angle(\text{O1-N1-N2-O2}) = 1.66^\circ$. Decomposition of the hyponitrite ligand in **1c*** explains the observed formation of N_2O and would also furnish dioxidorhenium(VII) complex **2**. The latter reacts with SMe_2 to give OSMe_2 , thereby regenerating **1**, which closes the catalytic cycle. The net reaction of $\mathbf{1} + 1 \text{ SMe}_2 + 2 \text{ NO} \rightarrow \mathbf{1} + \text{N}_2\text{O} + \text{OSMe}_2$ is also consistent with the observed conversion in the described stoichiometric reaction with NO_2^- forming 0.5 equivalents of SMe_2 to OSMe_2 (Fig. 2).

We assume this unusual reductive reactivity towards NO is due to the high oxidation state of Re(V) in **1**, which does not allow for the formation of a stable nitrosyl complex. The resulting species **1a*** is a $\{\text{ReNO}\}^3$ nitrosyl complex by the Enemark-Feltham notation [36]. High oxidation state Re-nitrosyl complexes have been rarely described in literature [37], and no examples of $\{\text{ReNO}\}^n$ complexes with $n \leq 4$ have been characterized by X-ray crystallography [38]. Also the lack of any stable intermediates observed computationally by going from **1b*** to **1c*** is reflecting the catalytic nature of this step.

3. Conclusions

A biomimetic, enzyme-like nitrate reduction catalyst has to be air- and water-stable, perform 1 and 2 e^- OAT steps and also accept gaseous substrates in the reduction sequence of NO_3^- to N_2 . Within this manuscript we provide ample evidence that Re(V) complex **1** does fulfill all these criteria. The thermodynamic most challenging reduction of nitrate to nitrite occurs catalytically via a 2 e^- OAT step. The subsequent reduction of nitrite occurs via a single electron transfer to yield catalytically inactive Re(VI) complex **2'** and gaseous NO. We could identify $[\text{Cu}(\text{II})\text{Cl}_2]$ as an efficient, simple and cheap 1 e^- oxidant capable to cleanly re-activate dioxidorhenium(VI) complex **2'**, allowing to also close the catalytic cycle of nitrite reduction. The formation of NO as the reduction product of NO_2^- was confirmed via gas-phase IR spectroscopy. In addition, we observed a unique Re-catalyzed NO reduction pathway via formation of a hyponitrite anion (**1c***), ultimately yielding N_2O . Such a further reduction of NO has not been observed for other nitrate reduction catalysts, as they usually form stable nitrosyl-complexes with NO. The high oxidation state of +V is the key feature in complex **1** to overcome this NO-poisoning. Due to the lack of π -backbonding, the formation of catalytically inactive nitrosyl complexes is avoided.

This further reduction of NO to N_2O opens the pathway to a rhenium-catalyzed full and selective reduction of nitrate to non-toxic N_2 , the ultimate goal in nitrate reduction. If also this last step to N_2 formation could be achieved, Re-complex **1** would fully mirror the biological, enzyme-catalyzed reduction of nitrate to N_2 .

CRedit authorship contribution statement

Fabian Wiedemaier: Conceptualization, Investigation, Writing – original draft. **David M. Köppler:** Data curation, Investigation. **Christian Schlegl:** Data curation, Investigation. **Christof Holzer:** Formal analysis, Methodology. **Ferdinand Belaj:** Investigation. **Nadia C. Mösch-Zanetti:** Writing – review & editing. **Jörg A. Schachner:** Conceptualization, Supervision, Writing – review & editing.

Funding

This research was funded in whole, or in part, by the Austrian Science Fund (FWF) [10.55776/P37178] (JAS). For the purpose of open access, the author has applied a CC BY public copyright license to any

Author Accepted Manuscript version arising from this submission. The authors also gratefully acknowledge support from NAWI Graz.

Declaration of competing interest

The authors declare that they have no known competing financial interests or personal relationships that could have appeared to influence the work reported in this paper.

Acknowledgement

We thank the following collaborators: Dr. Ph. Neu and Assoc. Prof. G. Raber from Institute of Chemistry, University of Graz, for acquiring ESI-MS spectra of **2'** and **3a**. Dr. D. Neshchadin (Institute of Physical and Theoretical Chemistry, Graz University of Technology) for several attempts to acquire an EPR spectrum of **2'**. We also thank Anton Paar GmbH for providing a prototype IR spectrometer “Lyza 7000 Beta” including a gas IR cell that was used in this research project.

Appendix A. Supplementary data

All data are available in the main text or the supplementary materials. Synthesis of complex $[\text{ReO}_2(\text{L1})_2]$ (**2'**) and isolation of complexes $[\text{ReO}(\text{L1})_2][\text{ReO}_4]$ (**3a**) ($\text{H}_2\text{L1}$)[ReO_4] (**3b**); ^1H NMR spectra of **2'**, **2**, **3a** and **3b**; oxidation of **1** by nitrate, comparison of UV-Vis spectra, Arrhenius plots for formation of **2** and decomposition to **3b**; table of pseudo-first order rate-constants of formation and decay of **2'**; cyclic voltammogram of **2'**; metadata is deposited at Zenodo under the DOI 10.5281/zenodo.15680876; details on crystallographic data acquisition and refinement as well as selected bond lengths and angles of **3a** and **3b** are given. CCDC 2172141 (**2'**), 2172142 (**3a**) and 2172143 (**3b**) contain the supplementary crystallographic data for this paper. This structure of **2'** is a polymorph to the previously published structure.[23] These data can be obtained free of charge from The Cambridge Crystallographic Data Centre via www.ccdc.cam.ac.uk/data_request/cif. Full experimental details for single-crystal X-ray diffraction analyses of both compounds are provided in the SM. Supplementary data to this article can be found online at <https://doi.org/10.1016/j.jcat.2025.116526>.

Data availability

Metadata has been deposited on Zenodo and will be made available upon acceptance of the manuscript. A link is shared in the manuscript

References

- [1] I.M. Wasser, S. de Vries, P. Moëne-Loccoz, I. Schröder, K.D. Karlin, Nitric oxide in biological denitrification. Fe/Cu metalloenzyme and metal complex NO x redox chemistry, *Chem. Rev.* 102 (2002) 1201–1234, <https://doi.org/10.1021/cr0006627>.
- [2] B. Kraft, M. Strous, H.E. Tegetmeyer, Microbial nitrate respiration—genes, enzymes and environmental distribution, *J. Biotechnol.* 155 (2011) 104–117, <https://doi.org/10.1016/j.jbiotec.2010.12.025>.
- [3] J.N. Galloway, F.J. Dentener, D.G. Capone, E.W. Boyer, R.W. Howarth, S. P. Seitzinger, G.P. Asner, C.C. Cleveland, P.A. Green, E.A. Holland, et al., Nitrogen cycles, past, present, and future, *Biogeochem.* 70 (2004) 153–226, <https://doi.org/10.1007/s10533-004-0370-0>.
- [4] a) B.A. Averill, Dissimilatory nitrite and nitric oxide reductases, *Chem. Rev.* 96 (1996) 2951–2964, <https://doi.org/10.1021/cr950056p>;
b) D.E. Canfield, A.N. Glazer, P.G. Falkowski, The evolution and future of Earth's nitrogen cycle, *Science* 330 (2010) 192–196, <https://doi.org/10.1126/science.1186120>.
- [5] N. Barrabes, J. Sá, Catalytic nitrate removal from water, past, present and future perspectives, *Appl. Catal. B: Environ.* 104 (2011) 1–5, <https://doi.org/10.1016/j.apcatb.2011.03.011>.
- [6] European Union (EU), Directive 2006/118/EC of the European Parliament and of the Council of 12 December 2006 on the protection of groundwater against pollution and deterioration. EUR-Lex - 02006L0118-20140711 - EN - EUR-Lex, can be found under <http://eur-lex.europa.eu/legal-content/EN/TXT/?uri=CELEX:02006L0118-20140711>, 2006.
- [7] a) M.H. Ward, B.A. Kilfoy, P.J. Weyer, K.E. Anderson, A.R. Folsom, J.R. Cerhan, Nitrate intake and the risk of thyroid cancer and thyroid disease, *Epidemiology* 21

- (2010) 389–395, <https://doi.org/10.1097/EDE.0b013e3181d6201d>;
- b) G. Gulis, M. Czompolyova, J.R. Cerhan, An ecologic study of nitrate in municipal drinking water and cancer incidence in Trnava District, Slovakia, *Environ. Res.* 88 (2002) 182–187, <https://doi.org/10.1006/enrs.2002.4331>.
- [8] J. Topich, Synthesis and reactions of polymer-anchored molybdenum(V and VI) tripeptide complexes, *Inorg. Chim. Acta* 46 (1980) L97–L100, [https://doi.org/10.1016/S0020-1693\(00\)84152-3](https://doi.org/10.1016/S0020-1693(00)84152-3).
- [9] a) S. Hörold, K.-D. Vorlop, T. Tacke, M. Sell, Development of catalysts for a selective nitrate and nitrite removal from drinking water, *Catal. Today* 17 (1993) 21–30, [https://doi.org/10.1016/0920-5861\(93\)80004-K](https://doi.org/10.1016/0920-5861(93)80004-K);
- b) K.-D. Vorlop, T. Tacke, Erste Schritte auf dem Weg zur edelmetallkatalysierten Nitrat- und Nitrit-Entfernung aus Trinkwasser, *Chem. Ing. Tech.* 61 (1989) 836–837, <https://doi.org/10.1002/cite.330611023>;
- c) S. Hörold, T. Tacke, K.-D. Vorlop, Catalytic removal of nitrate and nitrite from drinking water: 1. Screening for hydrogenation catalysts and influence of reaction conditions on activity and selectivity, *Environ. Technol.* 14 (1993) 931–939, <https://doi.org/10.1080/09593339309385367>.
- [10] J. Martínez, A. Ortiz, I. Ortiz, State-of-the-art and perspectives of the catalytic and electrocatalytic reduction of aqueous nitrates, *Appl. Catal. B: Environ.* 207 (2017) 42–59, <https://doi.org/10.1016/j.apcatb.2017.02.016>.
- [11] B.P. Chaplin, M. Reinhard, W.F. Schneider, C. Schüth, J.R. Shapley, T. J. Strathmann, C.J. Werth, Critical review of Pd-based catalytic treatment of priority contaminants in water, *Environ. Sci. Technol.* 46 (2012) 3655–3670, <https://doi.org/10.1021/es204087q>.
- [12] a) U. Prüsse, M. Hähnlein, J. Daum, K.-D. Vorlop, Improving the catalytic nitrate reduction, *Catal. Today* 55 (2000) 79–90, [https://doi.org/10.1016/S0920-5861\(99\)00228-X](https://doi.org/10.1016/S0920-5861(99)00228-X);
- b) S. Guo, K.N. Heck, S. Kasiraju, H. Qian, Z. Zhao, L.C. Grabow, J.T. Miller, M. S. Wong, Insights into nitrate reduction over indium-decorated palladium nanoparticle catalysts, *ACS Catal.* 8 (2018) 503–515, <https://doi.org/10.1021/acscatal.7b01371>.
- [13] J. Liu, J.K. Choe, S. Sasnow, C.J. Werth, T.J. Strathmann, Application of a Re–Pd bimetallic catalyst for treatment of perchlorate in waste ion-exchange regenerant brine, *Water Res.* 47 (2013) 91–101, <https://doi.org/10.1016/j.watres.2012.09.031>.
- [14] M.M. Abu-Omar, E.H. Appelman, J.H. Espenson, Oxygen-transfer reactions of methylrhodium oxides, *Inorg. Chem.* 35 (1996) 7751–7757, <https://doi.org/10.1021/ic960701q>.
- [15] A. Majumdar, K. Pal, S. Sarkar, Chemistry of $\text{Et}_4\text{NMo}^{\text{IV}}(\text{SPh})(\text{PPh}_3)(\text{mnt})_2$ as an analogue of dissimilatory nitrate reductase with its inactivation on substitution of thiolate by chloride, *J. Am. Chem. Soc.* 128 (2006) 4196–4197, <https://doi.org/10.1021/ja0586135>.
- [16] C.L. Ford, Y.J. Park, E.M. Matson, Z. Gordon, A.R. Fout, A bioinspired iron catalyst for nitrate and perchlorate reduction, *Science* 354 (2016) 741–743, <https://doi.org/10.1126/science.aah6886>.
- [17] a) J.M. Moore, T.J. Miller, M. Mu, M.N. Peñas-Defrutos, K.L. Gullett, L.S. Elford, S. Quintero, M. García-Melchor, A.R. Fout, Selective stepwise reduction of nitrate and nitrite to dinitrogen or ammonia, *J. Am. Chem. Soc.* 147 (2025) 8444–8454, <https://doi.org/10.1021/jacs.4c16585>;
- b) M.D. Lim, I.M. Lorkovic, P.C. Ford, Kinetics of the oxidation of triphenylphosphine by nitric oxide, *Inorg. Chem.* 41 (2002) 1026–1028, <https://doi.org/10.1021/ic0108585>.
- [18] M.A. Ehweiner, F. Wiedemaier, F. Belaj, N.C. Mösch-Zanetti, Oxygen atom transfer reactivity of Molybdenum(VI) complexes employing pyrimidine- and pyridine-2-thiolate ligands, *Inorg. Chem.* 59 (2020) 14577–14593, <https://doi.org/10.1021/acs.inorgchem.0c02412>.
- [19] a) J.M. Moore, A.R. Fout, Synthetic strategies for oxyanion reduction: Metal-based insights and innovations, *Coord. Chem. Rev.* 541 (2025) 216692, <https://doi.org/10.1016/j.ccr.2025.216692>;
- b) B. Tran, J. Smith, Nitrogen oxyanion deoxygenation: Redox chemistry and oxygen atom transfer reactions, *Coord. Chem. Rev.* 530 (2025) 216490, <https://doi.org/10.1016/j.ccr.2025.216490>.
- [20] J. Gwak, S. Ahn, M.-H. Baik, Y. Lee, One metal is enough: a nickel complex reduces nitrate anions to nitrogen gas, *Chem. Sci.* 10 (2019) 4767–4774, <https://doi.org/10.1039/c9sc00717b>.
- [21] A.W. Beamer, J.A. Buss, Surface-like NO_x reduction at an atomically-precise tricopper cluster, *Angew. Chem. Int. Ed.* 64 (2025) e202424772, <https://doi.org/10.1002/anie.202424772>.
- [22] J.A. Schachner, B. Terfass, L.M. Peschel, N. Zwettler, F. Belaj, P. Cias, G. Gescheidt, N.C. Mösch-Zanetti, Oxorhenium(V) complexes with phenolate–oxazoline ligands, *Inorg. Chem.* 53 (2014) 12918–12928, <https://doi.org/10.1021/ic501932c>.
- [23] J.A. Schachner, F. Wiedemaier, N. Zwettler, L.M. Peschel, A.D. Boese, F. Belaj, N. C. Mösch-Zanetti, Catalytic reduction of nitrate by an oxidorhenium(V) complex, *J. Catal.* 397 (2021) 108–115, <https://doi.org/10.1016/j.jcat.2021.03.028>.
- [24] L. Alig, K.A. Eisenlohr, Y. Zelenkova, S. Rosendahl, R. Herbst-Irmer, S. Demeshko, M.C. Holthausen, S. Schneider, Rhenium-mediated conversion of dinitrogen and nitric oxide to nitrous oxide, *Angew. Chem. Int. Ed.* 61 (2021) e202113340, <https://doi.org/10.1002/anie.202113340>.
- [25] D.D. DuMez, J.M. Mayer, Synthesis and characterization of Rhenium(VI) cis-dioxo complexes and examination of their redox chemistry, *Inorg. Chem.* 37 (1998) 445–453, <https://doi.org/10.1021/ic9710317>.
- [26] S. Fukuzumi, K. Shimoosako, T. Suenobu, Y. Watanabe, Mechanisms of hydrogen-, oxygen-, and electron-transfer reactions of cumylperoxyl radical, *J. Am. Chem. Soc.* 125 (2003) 9074–9082, <https://doi.org/10.1021/ja035156o>.
- [27] R.H. Gillette, E.H. Eyster, The fundamental rotation-vibration band of nitric oxide, *Phys. Rev.* 56 (1939) 1113–1119, <https://doi.org/10.1103/PhysRev.56.1113>.
- [28] K.-M. Roy in *Ullmann's encyclopedia of industrial chemistry*, in: M. Bohnet (Ed.), Wiley-Interscience, 1999.
- [29] H. Tsukahara, T. Ishida, M. Mayumi, Gas-phase oxidation and disproportionation of nitric oxide, *Methods Enzymol.* 359 (2002) 168–179.
- [30] a) R. Eisenberg, C.D. Meyer, Coordination chemistry of nitric oxide, *Acc. Chem. Res.* 8 (1975) 26–34, <https://doi.org/10.1021/ar50085a004>;
- b) P.C. Ford, I.M. Lorkovic, Mechanistic aspects of the reactions of nitric oxide with transition-metal complexes, *Chem. Rev.* 102 (2002) 993–1018, <https://doi.org/10.1021/cr0000271>.
- [31] N. Mardirossian, M. Head-Gordon, ωB97M-V: a combinatorially optimized, range-separated hybrid, meta-GGA density functional with VV10 nonlocal correlation, *J. Chem. Phys.* 144 (2016) 214110, <https://doi.org/10.1063/1.4952647>.
- [32] C. Holzer, Y.J. Franzke, A general and transferable local hybrid functional for electronic structure theory and many-fermion approaches, *J. Chem. Theory Comput.* 21 (2025) 202–217, <https://doi.org/10.1021/acs.jctc.4c01309>.
- [33] S. Kundu, P.N. Phu, P. Ghosh, S.A. Kozimor, J.A. Bertke, S.C.E. Stieber, T. H. Warren, Nitrosyl linkage isomers: NO coupling to N₂O at a mononuclear site, *J. Am. Chem. Soc.* 141 (2019) 1415–1419, <https://doi.org/10.1021/jacs.8b09769>.
- [34] J.A. Olabe, L.D. Slep, *Comprehensive Coordination Chemistry II. From Biology to Nanotechnology*, Elsevier, Pergamon, Amsterdam, 2004.
- [35] A.M. Wright, H.T. Zaman, G. Wu, T.W. Hayton, Mechanistic insights into the formation of N₂O by a nickel nitrosyl complex, *Inorg. Chem.* 53 (2014) 3108–3116, <https://doi.org/10.1021/ic403038e>.
- [36] J.H. Enemark, R.D. Feltham, Principles of structure, bonding, and reactivity for metal nitrosyl complexes, *Coord. Chem. Rev.* 13 (1974) 339–406, [https://doi.org/10.1016/S0010-8545\(00\)80259-3](https://doi.org/10.1016/S0010-8545(00)80259-3).
- [37] a) A.R. Middleton, G. Wilkinson, Further studies on the interaction of nitric oxide with transition-metal alkyls, *J. Chem. Soc., Dalton Trans.* 9 (1981) 2081–2096, <https://doi.org/10.1039/dt9810001898>;
- b) A. Gutierrez, G. Wilkinson, B. Hussain-Bates, M.B. Hursthouse, t-Butylimido and t-butylimido oxo aryls of rhenium. X-ray crystal structures of $\text{Re}(\text{NBut})_2(2,6\text{-Me}_2\text{C}_6\text{H}_3)_2$, $\text{Re}(\text{NBut})(2,4,6\text{-Me}_3\text{C}_6\text{H}_2)(\text{C}_2\text{H}_3\text{H}_3)$, $\text{Re}(\text{NBut})_3(2,4,6\text{-Me}_3\text{C}_6\text{H}_2)$, $[(\text{ButN})\text{Br}(2,4,6\text{-Me}_3\text{C}_6\text{H}_2)\text{Re}(\mu\text{-NBut})(\mu\text{-O})(\text{OC}_6\text{H}_2\text{Me}_2\text{CH}_2)(\text{NBut})]$, $[\text{Re}(\text{NBut})(\text{OAr}(\mu\text{-O}))_2]$, Ar = 2,6-C₆H₃ and 2,4,6-C₆H₂, *Polyhedron* 9 (1990) 2081–2096, [https://doi.org/10.1016/S0277-5387\(00\)84039-5](https://doi.org/10.1016/S0277-5387(00)84039-5).
- [38] a) B. Machura, Structural and spectroscopic properties of rhenium nitrosyl complexes, *Coord. Chem. Rev.* 249 (2005) 2277–2307, <https://doi.org/10.1016/j.ccr.2005.03.022>;
- b) J.R. Dilworth, Rhenium chemistry – then and now, *Coord. Chem. Rev.* 436 (2021) 213822, <https://doi.org/10.1016/j.ccr.2021.213822>.